uc3m | Universidad Carlos III de Madrid

Department of Aerospace Engineering

2017-2018

Bachelor Thesis

"Simulation and pre-design of a controlled super-pressure balloon"

Isaac Ramsés Buitrago Ramos

Tutor

Manuel Sanjurjo Rivo

June 19, 2018

ABSTRACT

In this document a deep study of the trajectory of a weather balloon is developed. Making use of a simulator coded in Matlab, it will be possible to predict the flight path prior launch.

The starting point is a pre-existing code which assumes that the properties inside the balloon are the same as in the outside; the first part of the project focuses on integrating the formulas needed to compute the temperature and pressure inside, together with the appropriate radius evolution.

The simulator will make use of an external data supplier, NOAA, which will provide the wind data based on predictions.

The second part of the project is devoted to make an experimental launch: once the system has been recovered and the data measured has been analyzed, a comparison between the simulator and the data obtained from the experiment can be done. The real trajectory of the balloon will be reconstructed from the data measured by the GPS.

DEDICATION:

I would like to express my gratitude to Manuel Sanjurjo, for his guidance and continuous support during the whole thesis. I would also like to be grateful to Guillermo Asensio, for his infinite patience and endless assistance since the beginning, which has made him become the "second tutor" of the project.

I would also like to dedicate this project to my familiy: each and every one of them has helped me during these years, no matter the circumstances.

Besides I cannot forget my friends, whose sense of humor has combined perfectly with mine to create countless good moments.

Finally, I would like to give special thanks to: Juan Carlos Nieto Sierra (for helping in the antennas based communication system and the development of the experiment), Carlos Cobos Pérez (for helping in the construction of the payload), Xin Chen (for helping in refining the arduino codes) and Gorka Castaño Lorenzo and Daniel Sánchez-Biezma Zarco (for helping in performing the tests).

CONTENTS

LIST OF FIGURES

LIST OF TABLES

1. INTRODUCTION

The first successful attempts to fly made by human beings were based on balloons; however, their initial purpose was eclipsed by the emergence and later development of aircraft. This event pushed the use of balloons into another direction, more scientific, that has been refined and improved since then. Also, recreational use has been always present in ballooning.

The idea to use a lighter than air gas in order to rise into the air started to be developed in 1764, by Jospeh Black, who demonstrated that a balloon filled with only hydrogen will rise (during the following two years, Henry Cavendish and Tiberius Cavallo joined to the Black's work). After that, more people began working and designing hydrogen balloons: i.e. the first hydrogen-filled balloon in the history was launched on August 27, 1783 in Paris, by Jacques Charles and the Robert brothers, and a few days later, the Montgolfier brothers were able to design the first manned balloon. Two years later, in 1785, two important events happenned: Jean-Pierre Blanchard flew across the English Channel (adding control to the balloon), and the town of Tullamore (Ireland) suffered what is considered the first disaster in aviation: a hot air balloon snagged on a chimney while taking-off, which made it crash into several houses and start a fire that burned part of the town.

The next century, in 1852, Henri Giffard flew the first steerable balloon (also known as blimp or dirigible), powered by a steam engine. Even though they were slow, their popularity grew, and was significant enough to compete with ships in the transportation field during the Second World War. However, on May 6, 1937, the airship LZ 129 Hidenburg caught fire, and 35 people died in the accident; the repercussion was so high that the presence of balloons for transportation vanished.

In the military field, the use of balloons was important during the Second World War, but they were gradually replaced by aircraft; although balloons were still used for observation. Nowadays, the use of balloons has focussed mainly in recreational transportation, advertising and scientific research.

In the last few years drones have substituted balloons in some applications at low altitudes that need a really precise control, but there are still a lot of projects and applications in which scientific balloons are essential, such as near space experiments. Thus, understanding the physics and all the elements that take place in the flight of balloons may help in optimizing everything involved in the launches (trajectory prediction, launch platform, tracing system, and so on), which means a reduction in costs and, consequently, an increase in the number of applications.

1.1. Motivation

As stated before, there are some applications in which balloons are necessary; the most interesting one (and probably the most ambitious) is near space experimentation. Even though this kind of experiments can be performed by sending the equipment to the International Space Station, if the budget is a leading issue, the possibility of doing them with a weather balloon based system becomes the best alternative. The topic of the budget will be discussed later in this document, but as a first approach, the total cost of materials of the project is around 600 €. Only with the addition of a platform including everything needed to perform the experiment and an altitude controller (super-pressure), a full operational system could be achieved. Finally, in the case of a substantial increase in the altitude and/or the duration of the mission, a system based on fleet of balloons might be implemented.

One of the most relevant application that is currently in development is Googles's Project Loon, whose purpose is to provide internet connection where there is lack of satellite reception. Moreover, NASA has several projects that use high altitude balloons: SuperTIGER Balloon, BETTII and Eclipse Balloon (all of them will be seen in more details in the section *State of art*).

Another use of balloons is the monitoring of air pollution: the study made by James A. Armstrong, Philip A. Russell, Leslie E. Sparks and Dennis C. Drehmel **[2]** showed that tethered balloons can be used to sample the air very accurately. This method is particularly useful because of the high movility: sampling can be performed at different altitude levels and locations (near the source), and for long periods of time. Although nowadays it is not the most popular technique, it might be a good alternative in the future.

Nevertheless, despite all the studies and promising projects involving weather balloons, the most important use is meteorological data acquisition (temperature, humidity, wind, etc.). This information is crucial for many companies, even the governments, and the majority of suppliers make use of high altitude balloons due to the simplicity and affordability of the launch.

1.2. State of art

In this section, the most important current projects in which balloons play the main role are going to be explained:

1.2.1. Google's Project Loon

[3] Its purpose is to provide internet connection wherever it cannot be achieved with satellite connection, making use of a fleet of weather balloons that floats at altitudes of approximately 20km; the layers with different predictable wind directions of the strato-

sphere, together with low velocities, make such altitudes ideal for this aim. The idea is to first determine where the balloon will be placed, and then put it in the altitude in which the wind will move the balloon where it is needed. The electronics are fed by solar panels (batteries are also included to ensure the contituous function), and the balloons incorporate a recovery system in order to facilitate their replacement once their useful life is over.

Fig. 1.1. Balloon of the project Loon

1.2.2. SuperTIGER Balloon

[8] It stands for Super Trans-Iron Galactic Element Recorder Balloon, and its goal is to collect information on cosmic rays (high-energy particles) from beyond the solar system. The balloon was launched in Antartica, and it has the record of longest flight of heavy-lift scientific balloons, with a duration of 55 days, and at an altitude close to 40km. SuperTIGER was designed in order to look for the most uncommon elements, those with heavy nuclei: the ultra-heavy cosmic ray. The SuperTIGER is able to detect the cosmic rays more accurately than any other ground detector, since it floats over 99% of the atmosphere, much closer to the colision of the cosmic ray with the atmospheric gas, so most of the losses due to the interaction of the particles cascade with the surroundings is avoided.

Fig. 1.2. SuperTIGER Balloon, in Antartica

1.2.3. Eclipse Balloon

[9] In order to have a wide record of the last solar eclipse (August 21, 2017), NASA launched a collaboration project with students across the United States. Besides the opportunity of the students to get used to the scientific method and astrobiology, there was a deeper objective for NASA: study the effect of Mars-like conditions on life. The Mars atmosphere is thinner and cooler than Earth's, and with more radiation, so the upper part of the stratosphere during a solar eclipse resembles the condition of Mars atmosphere.

NASA provided each team with a pair of small metallic cards with bacteria dried on the surface; one would fly with the balloon while the remaining one would stay on the ground. After the flight, both cards were compared to see the consequences in the bacteria of being exposed to Mars-like environment.

1.2.4. BETTII

[7] It stands for Balloon Experimental Twin Telescope for Infrared Interferometry, and it is a balloon-borne far-infrared interferometer. It combines an 8-meter baseline with a double-Fourier Michelson interferometer, which allows the obtainment of both spatial and spectral information at the same time. The main characteristic of BETTII that highlights over single aperture telescopes (these have been the preferred option to make far-infrared, FIR, astronomy observations) is the increase in angular resolution without needing a higher aperture size. This technique has been improved and refined since the first prototypes were designed, and it seems that will it be essential in the future of space observation, which makes high altitude balloons a key factor in this field.

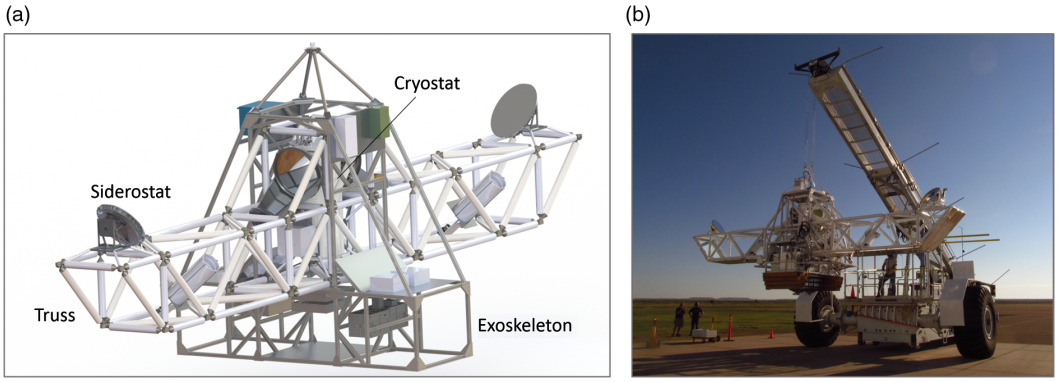

Fig. 1.3. Scheme (a) and prototype (b) of BETTII

1.3. Objectives

The main goal of this project is to compare the results of a real launch with those predicted with a numerical simulator coded in Matlab. The part of the simulator will have two phases: depuration and refinement of an existing code that makes some simplifications in terms of temperature and material evolution, and the incorporation of physical laws to the same code in order to properly determine those variables. The experimental results will be compared to both phases of the simulator, so that the improvement of the model can be appreciated.

Afterwards, the simulator will be revised in order to find the possible sources of error so that the prediction of the trajectory of a second launch (that will be done if the time allows us to do it) is closer to reality. It is important to take into account that the simulator is based on wind predictions supplied by an external source, which will introduce uncontrolled uncertainty in the system.

Once the experimental and optimization process have been performed, the posibility of including control to the balloon will be explored:

- In terms of the experiment, the means of obtaining the control, and what modifications must be done to the actual system.
- In terms of the simulation, see if the model fits with a super-pressure balloon, and in the case it does not, how to implement the control in the code.

Although this project does not go further, it will provide enough knowledge about balloon science to understand and detect what are the key parameters in a flight, and depending on the mission, how to optimize the system.

1.4. Future applications

This project is just the beginning of what should end up in a complete system based on a super-pressure balloon. Apart from all the current uses mentioned before in this document, there are two applications that could benefit from high altitude balloons: wildfire detection and border control.

1.4.1. Wildfire detection

Nowadays no wildfire detection system exists but those based on visual detection, which usually issue an alert too late to really avoid severe losses. In Spain, around 96% of them are provoked by the human being. However, decreasing that percentage to values close to zero will be only possible in a far future.

It is possible to reduce the time response to a wildfire by making use of several high altitude balloons positioned in areas that are more prone to start a fire. With the proper equipment (temperature and humidity sensors, infrared cameras...), the balloons could be able to warn before the fire has gone out of control, saving not only flora and fauna, but also money in damage reparation (mainly reforestation).

1.4.2. Border control

Another possbile application is the border control in the sea. Due to its geographic location, most of the drug trafficking in Spain comes from the sea: Galician coast, Mediterranean coast and Strait of Gibraltar.

The Spanish border control has a fleet of ships that patrol the seas, but they cannot cover the whole coast. Besides they also use unmanned helicopters and drones equipped with infrared and high quality cameras, but these devices do not fly for long periods of time. If some of them are substitued by balloons with some kind of horizontal control, the most critical areas could be in full-time surveillance (in normal conditions, super-pressure balloons can float during months).

1.5. Time planning

The main tasks developed through this project were: research and study of the bibliography, refinement of the Matlab simulator, addition of temperature and material evolution to the Matlab simulator, Arduino coding of the electronics, assembly of the electronics, assembly of the payload, tests, execution of the experiment and writing of the thesis.

TABLE 1.1. TIME PLANNING

Task	Estimated working hours
Research	84
Simulator refinement	24
Simulator improve	84
Arduino coding	72
Electronics assembly	12
Payload assembly	24
Tests	48
Experiment	36
Writing	100
Total	484

1.5.1. Engineer salary

According to the last regulation about the salary of newly graduated engineers **[19]**, a rough estimation of the payment for doing this project can be made: being the salary 1687.02 €/month, with 4 weeks per month and assuming 40 working hours per week, the salary per hour would be 10.54 €/h approximately. Taking into account the amount of hours dedicated to the project, which are about 484 h, the corresponding payment would be 5101.36 €.

1.6. Budget

This section is devoted to show the estimated cost of the project. As it has been mentioned before in this chapter (in the *Methodology*), this is a very important issue because the lower is the amount of money needed to perform the experiment, the easier will be to take advantage of it in terms of affordability.

TABLE 1.2. COST OF THE MATERIALS

Object	**Quantity**	**Price per unit [€/unit]**	**Total price [€]**
ELECTRONICS			
Arduino UNO R3	2	9.99	19.98
Adafruit GPS	1	51.74	51.74
NTX2B (434.650 MHz)	1	31	31
Resistor	4	0.05	0.20
SD card (2 GB)	2	3	6
Buzzer	1	7.99	7.99
Battery module	2	6.10	12.20
Cables	1	10.59	10.59
SD card reader (Arduino)	1	1.99	1.99
MinIMU-9 v5	1	13.50	13.50
DHT22 Sensor	1	9.05	9.05
Coaxial cable	1	14.08	14.08
Antenna cable	1	5.99	5.99
OTHERS			
Balloon (600 g)	2	50.96	101.92
Sport camera	3	20.99	62.97
Mini A8 GPS tracker	1	8.94	8.94
SIM card	1	20	20
Helium tank	1	40	40
Power bank	3	11.92	35.76
Batteries (20 per box)	2	9.78	19.56
Ground antenna	1	71.40	71.40
Parachute	1	7.99	7.99
Carabiner	1	3.90	3.90
Rope (50 m)	1	19.99	19.99
Belts	1	9.30	9.30
Total budget			586.04 €

2. REGULATIONS

Before the launch, there are some requirements according to regulations, established in Europe by the Civil Aviation Authority **[13] [14]** in the part of unmanned free balloons, that must be fulfilled. The most important for this project are mainly related to: classification, operating rules, limitations and equipment, termination, flight notification, position recording and super-pressure balloons.

2.1. Classification of unmanned free balloons

Unmanned free balloons are classified as:

a) Light: payload of one or more packages with a combined mass of less than 4 kg.

b) Medium: payload of two or more packages with a combined mass between 4 kg and 6 kg.

c) Heavy: payload which:

- has a combined mass of 6 kg or more; or
- includes a package of 3 kg or more; or
- includes a package of 2 kg or more with an area density of more than 13 g per square centimetre, determined by dividing the total mass in grams of the payload package by the area in cm^2 of its smallest surface; or
- uses a rope or other device for suspension of the payload that requires an impact force of 230 N or more to separate the suspended payload from the balloon.

2.2. General operating rules

1. Any balloon must not be operated without authorization from the State from which the launch is made and the States it crosses during the mission.
2. The authorization mentioned in the previous paragraph has to be obtained prior to the launch.
3. Any balloon must include the necessary means in order to avoid damage of any of its components when they impact on the earth.
4. A heavy balloon flying over the seas must be operated with coordination with the ANSP(s).

2.3. Operating limitations and equipment requirements

1. A heavy balloon must not be operated without authorization at or below 18000 m altitude if the visibility is low (due to clouds or any other darking phenomena).

2. A heavy or medium balloon must not fly at heights below 300 m over any congested area.

3. A heavy balloon must not be operated unless:

   a) it includes at least two payload flight-termination devices, no matter if they are automatic or telecommanded, that can work independently of each other;

   b) the balloon's envelope is equipped with either a radar reflective device or material that will allow the continuous tracking from a ground radar.

4. A heavy balloon must not be operated under the following conditions:

   a) in an area where ground-based SSR equipment is used, unless it contains a secondary surveillance radar transponder; or

   b) in an area where ground-based ADS-B equipment is used, unless it contains an ADS-B transmitter.

5. A heavy balloon must not fly below 18000 m altitude at night unless the balloon and its parachute (if any) are equipped with a light of any kind.

2.4. Termination

A heavy balloon must get its termination devices activated:

a) when weather conditions are diverge enough from the ones expected;

b) if the prolongation of the mission will be hazardous to air traffic or ground; or

c) if it will cross an unauthorised State.

2.5. Flight notification

1. Pre-flight Notification.

   1.1. Early notification of the flight of any medium or heavy balloon must be notificated at east seven days before the launch.

   1.2. Notification of the flight must include such the following information:

      a) balloon flight identification if medium or heavy balloon;

b) balloon classification and description;
c) SSR code if heavy balloon;
d) operator's name and telephone number;
e) launch site;
f) estimated time of launch;
g) number of balloons to be launched and schedule (if more than one is launched);
h) expected direction of ascent;
i) cruising level(s) (pressure-altitude);
j) estimated elapsed time to reach 18000 m pressure-altitude, together with the approximate location;
k) estimated date and time of termination of the flight and the planned location of the impact on the ground.

1.3. Any changes in the pre-launch information must be notified not less than 6 hours before the estimated time of launch.

2. Notification of Launch.

2.1. After a medium or heavy balloon is launched, the operator must inform of:

a) balloon flight identification;
b) launch site;
c) actual time of launch;
d) estimated elapsed time to reach 18000 m pressure-altitude, together with the approximate location;; and
e) any changes to the information previously notified.

3. Notification of Cancellation.

3.1. The operator must notify the appropriate ATS as soon as he or she knows that the flight of a medium or heavy balloon has been cancelled.

2.6. Position recording and reports

1. The operator of a heavy balloon flying at or below 18000 m altitude must monitor its path and reports its position every 2 hours.

2. The operator of a heavy balloon flying above 18000 m altitude must monitor its path and reports its position every 24 hours.

3. In the case that a position cannot be recorded, the operator must immediately notify the appropriate ATS the last recorded position and when the tracking has returned to normal.

4. The operator of a heavy balloon must inform one hour before the descent of:

   a) the current geographical position;

   b) the current altitude;

   c) the forecast time of crossing 18000 m of altitude (in the case that it will happen);

   d) the forecast time and location of ground impact.

5. The operator of a heavy or medium balloon must notify when the operation has finished.

2.7. Operating limitations and equipment requirements for super-pressure balloons

Super-pressure balloons do not require flight termination devices.

3. METHODOLOGY

The project is mainly divided into two parts. One is related with the implementation of the material and temperature evolution in a Matlab code, and the other one is devoted to the launch of a balloon to compare the results with the predictions made with the simulator.

3.1. Simulator

In order to simulate the flight trajectory of the balloon in an accurate way, it is necessary to implement some fundamental equations (i.e. buoyancy force and radial heat diffusion) in a Matlab code. This code will take as initial conditions: the weight of the payload, the parameters of the balloon (lifting gas quantity, enclosed volume and total weight inlcuding the latex film and the inner gas), and the location and atmospheric parameters (temperature and pressure) of the launch. Afterwards, the code will make use of some equations as the usual mathematical model: take some inputs, such as the altitude (temperature and pressure), to compute some outputs, such as the velocity in the 3 axis and the increase in volume inside the balloon.

The starting point is an existing code which already includes the first two parts: dynamic equations and wind data; although it is not the aim of the project, they will be briefly explained so that the basis is also present. This code is rough in the automation aspect, so the first modification will be related to automate the wind data gathering process. Furthermore, some simplifications regarding the temperature evolution will be modified to improve the model; another correction will be the exact calculation of the burst point, which the code is currently unable to predict.

3.1.1. Dynamic equations

The first step is to define an appropriate coordinate system **[1]**, which is the one depicted in *Figure 3.1*. Afterwards, the forces acting on a balloon can be determined: drag (parallel to the wind, $\vec{e_w}$), lateral (perpendicular to the wind, $\vec{e_p}$) and free-lift (it is the result of substracting the buoyancy force and the weight of the balloon):

$$\vec{F_D} = \frac{1}{2}\rho S\,|\vec{v_w} - \vec{v_b}|^2 C_D\ \vec{e_w} \tag{3.1}$$

$$\vec{F_Y} = \frac{1}{2}\rho S\,|\vec{v_w} - \vec{v_b}|^2 C_Y\ \vec{e_p} \tag{3.2}$$

$$\vec{F_{fl}} = (\rho_a V_b - m_t)\,g\ \vec{k} \tag{3.3}$$

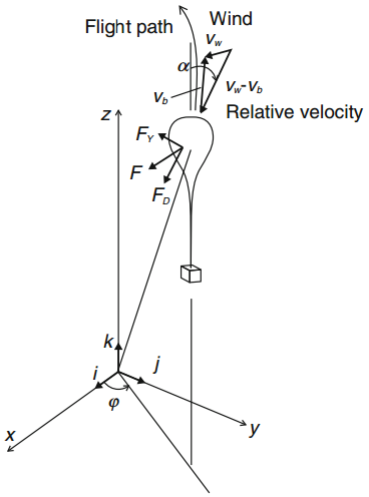

Fig. 3.1. Coordinate system

Regarding S in *Eqs 3.1 & 3.2*, it represents the reference area, which can be arbitrarily chosen. In the simulator, the reference area will be assumed as half of the external area of a sphere with the same volume as the balloon ($S = 2\pi R^2$). And with respect to the velocities, $\vec{v_w}$ denotes the wind velocity and $\vec{v_b}$ the velocity of the balloon (both of them are vectors with the 3 components corresponding to the axis of the coordinate system in *Figure 3.1*).

At this point, the angles that relate the velocity of the balloon and the absolute velocity can be defined as: α, the angle between the relative velocity ($\vec{v_w} - \vec{v_b}$) and the z-axis; and φ, the angle between the projection of the relative velocity onto the xy plane and the x-axis. With these angles, the three components of the aerodynamic forces acting on the balloon can be determined:

$$\vec{F_x} = (F_D sin\ \alpha + F_Y cos\ \alpha)\, cos\ \varphi\ \vec{i} \tag{3.4}$$

$$\vec{F_y} = (F_D sin\ \alpha + F_Y cos\ \alpha)\, sin\ \varphi\ \vec{j} \tag{3.5}$$

$$\vec{F_z} = -F_D cos\ \alpha + F_Y sin\ \alpha\ \vec{k} \tag{3.6}$$

The first assumption comes from the shape: the balloon will be considered as a perfect sphere that only deforms by augmenting the radius (and thus reducing the envelope thickness). The first implication of this assumption is that $C_Y = 0$, so $F_Y = 0$ as well. The other direct implication regards C_D, although it is not as simple as for the lateral coefficient.

The drag coefficient of a perfect sphere is mainly a function of two parameters: the Reynolds number, $Re = \rho_a R v_z / \mu$, and the free-stream turbulence intensity (Tu, in %), which is the ratio of the standard deviation of the incident air velocity fluctuations to the mean incident air velocity.

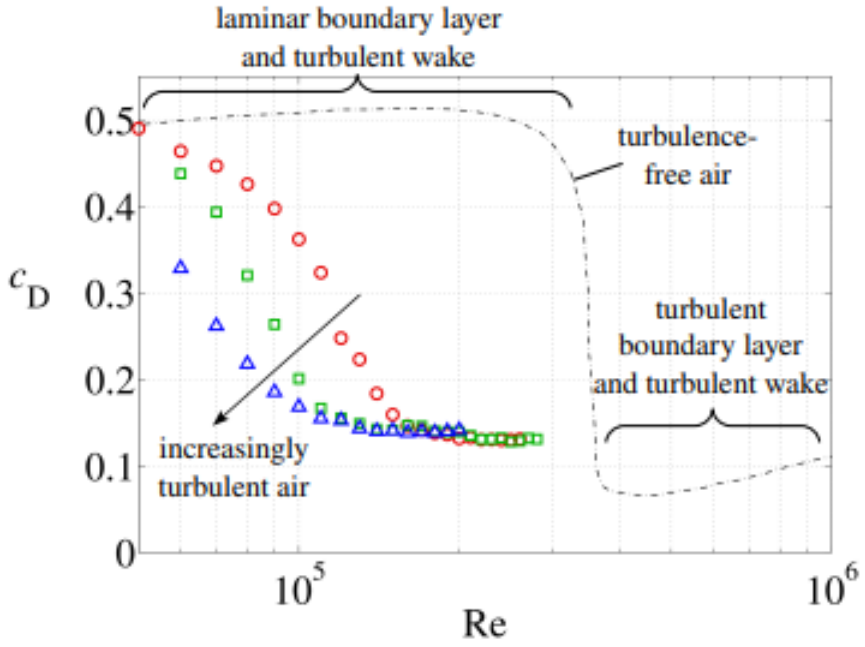

Fig. 3.2. Drag coefficient of a sphere as a function of Re: $Tu = 0.45\%$ (- -), $Tu = 4\%$ (red), $Tu = 6\%$ (green), $Tu = 45\%$ (blue)

The flight will be considered in low-turbulence (below 1 %) and in a range of low Reynolds number ($Re < 3 \cdot 10^5$), which means that C_D will not diverge much from 0.5.

Finally, a clarification about the masses needs to be done. The balloon system mass (m_G) will be the addition of the balloon mass (m_b), the payload mass (m_p) and the balloon's ballast (m_c):

$$m_G = m_b + m_p + m_c \tag{3.7}$$

If then the lifting gas mass (m_g) is added, the total mass of the system is obtained:

$$m_t = m_G + m_g \tag{3.8}$$

If at this point we consider the virtual mass ($m_{virt} = C_m \rho_a V_b$; the value of C_m for a perfect sphere is assumed to be 0.5), which is the mass of air dragged:

$$m_v = m_t + m_{virt} \tag{3.9}$$

This is the mass that will be used in the equations of Newton's second law:

$$m_v \frac{d^2 \vec{x_b}}{dt^2} = \vec{F_x} \tag{3.10}$$

$$m_v \frac{d^2 \vec{y_b}}{dt^2} = \vec{F_y} \tag{3.11}$$

$$m_v \frac{d^2 \vec{z_b}}{dt^2} = \vec{F_{fl}} + \vec{F_z} \tag{3.12}$$

3.1.2. Wind data: NOAA

The wind data is provided by the National Oceanic and Atmospheric Administration (NOAA), which is a scientific company that analyzes atmospheric and oceanic conditions. The information that NOAA gathers is available in its webpage for anyone interested. From all the models that NOAA offers, the one that will be used in this project is the Global Forecast System (GFS).

The GFS is a weather forecast model produced by the National Centers for Environmental Prediction (NCEP). Many atmospheric variables are available through this dataset, such as temperature, humidity and wind. The globe is gridded in a way that a resolution of 28 km is obtained, and the predictions extend to 16 days into the future, with a prediction issued every 3 hours.

It is important to notice that the predictions vary from day to day, being the closer to reality the prediction made just the day before. In order to see how the solution will be affected by this factor, the simulator will be run with different predictions to compare the results. Furthermore, as it was mentioned before in this document (section *3.1. Simulator*), the refinement of the existing code is focused mainly in automating the process of collecting the forecast data: the polished code will download automatically the desired file from the webpage (instead of having to do it manually).

3.1.3. Temperature equations

At this point, the formula that defines the volume of the balloon is:

$$V_b = \frac{m_g}{W_g}\frac{R_u T_{in}}{P_{in}} \tag{3.13}$$

where the subscript "in" refers to inside, W_g is the molecular weight of the lifting gas (helium in this case) and $R_u = 8.314\ J/molK$. However, another assumption made in the simulator was that the temperature inside is the same as in the outside. This simplification will be corrected in this project, making use of the heat diffusion equation.

The reason why a balloon bursts when it reaches high altitudes is a decrease in the thickness beyond the limit of the material, due to a radius increase and volume conservation. This variation in the radius occurs due to both adiabatic expansion and heat transfer from the surrounding air into the balloon. Furthermore, this model will only account for diffusion as the way to propagate the heat flux; it means that both eddy (turbulent) diffusion and convection are not included since they do not play an important role.

The temperature distribution inside the balloon, which is assumed to be spherically simmetrical, will be computed using the radial heat diffusion equation **[4] [15]**:

$$\frac{\partial T_b}{\partial t} = \frac{\bar{D}}{R^2}\frac{1}{r^2}\frac{\partial}{\partial r}\left(r^2\frac{\partial T_b}{\partial r}\right) \tag{3.14}$$

where T_b $(= T_{in})$[1] is the temperature inside the balloon, R is the balloon effective radius, t is time and $r \epsilon [0, 1]$ is the non-dimensional radial coordinate.

The last parameter of *Eq. 3.14* is the average of the mean molecular heat diffusion coefficient:

$$\bar{D} = \frac{\bar{\kappa}}{\rho_b \bar{c}_p} \tag{3.15}$$

In this equation, ρ_b can be easily calculated using the ideal gases formula:

$$\rho_b = \frac{m_g}{V_b} = \frac{3m_g}{4\pi R^3} \, , \tag{3.16}$$

and $\hat{\kappa}$ and $\hat{c}_p$ are the averaged thermal conductivity and specific heat capacity of the lifting gas, respectively. Although both variables vary with temperature, the change in c_p is so small that it will be assumed to be constant with the value at 300K: $c_{p_{300K}} = \hat{c}_p = 5192.6 \; J/kgK$. For the case of the thermal conductivity:

TABLE 3.1. THERMAL CONDUCTIVITY OF HELIUM

Temperature [K]	$\kappa \; [W \cdot m^{-1} \cdot K^{-1}]$
100	0.0755
200	0.1193
300	0.1567
400	0.1906
500	0.2223
600	0.2525

Since the range of temperatures at which the balloon will be exposed goes from 200K to 300K (approximately), it will be ok to assume a constant value for the thermal conductivity of: $\hat{\kappa} = 0.13 \; W/mK$. This will imply that the heat diffusion coefficient will only change because of the density (pressure and temperature).

The boundary conditions of *Eq. 3.14* are: the temperature inside at the surface of the balloon is equal to the temperature outside, $T_b(r = 1) = T_{out}$, and the heat flux at the center of the balloon is zero due to symmetry, $(\partial T_b / \partial r)_{r=0} = 0$.

At this point, it is possible to simplify *Eq. 3.14* because the expansion terms are not considered; the simplification would be equivalent to consider the lifting gas as incompressible, which means that the balloon effective radius keeps constant while heat diffusion occurs, as well as the heat diffusion coefficient. This restriction is valid for small time intervals (0.3-1s), but it is also possible to make a correction accounting for this simplification at the end of each time interval.

[1] Along this document, the temperature inside the balloon will be referred to as T_{in} and T_b.

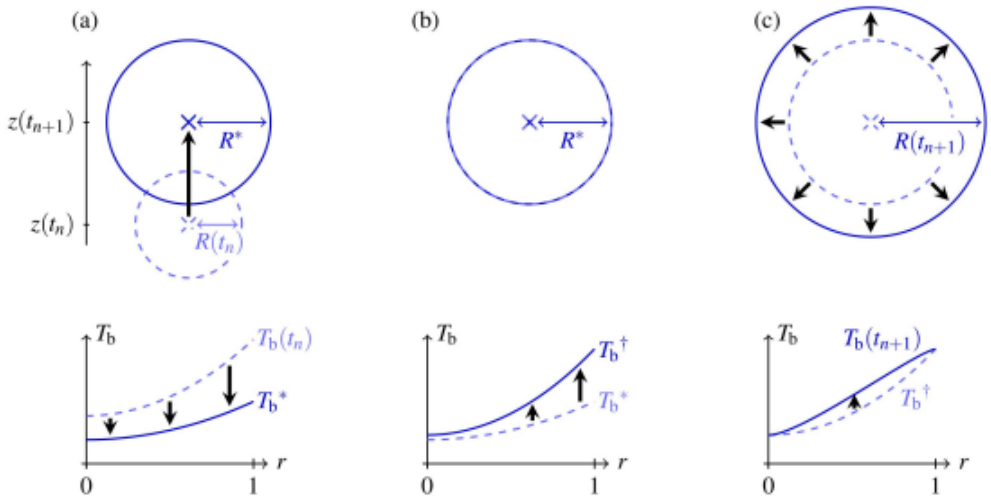

Fig. 3.3. Stages of the balloon effective radius variation from t_n to t_{n+1}. **(a)** Adiabatic expansion. **(b)** Heat diffusion at constant pressure. **(c)** Correction

The best model to solve this problem includes several steps (this model was developed for balloons in still air, so it could not be directly applied to our project unless the wind is taken into account). The time step is denoted by Δt and the increase in altitude by Δz, and they are related by: $\Delta z = v_z \Delta t + O(\Delta t^2)$. A single step of the model contains two parts:

1. The calculation of the balloon effective radius (R) and the temperature inside (T_b) at time $t + \Delta t$ using the values at time t.
2. The calculation of the drag coefficient and the vertical velocity of the balloon at time $t + \Delta t$ with the following formula:

$$v_z = \sqrt{\frac{8Rg}{3c_D}\left(1 - \frac{3m_t}{4\pi\rho_a R^3}\right)} \tag{3.17}$$

As it can be seen in *Figure 3.3*, the computation of the balloon effective radius of part 1 is divided in three steps:

(a) Adiabatic expansion of the balloon from altitude $z(t_n)$ to $z(t_{n+1})$.

(b) Heat diffusion inside the balloon at constant pressure.

(c) Correction to the balloon effective radius and temperature distribution.

In *Figure 3.4* a more detailed diagram of the model is depicted:

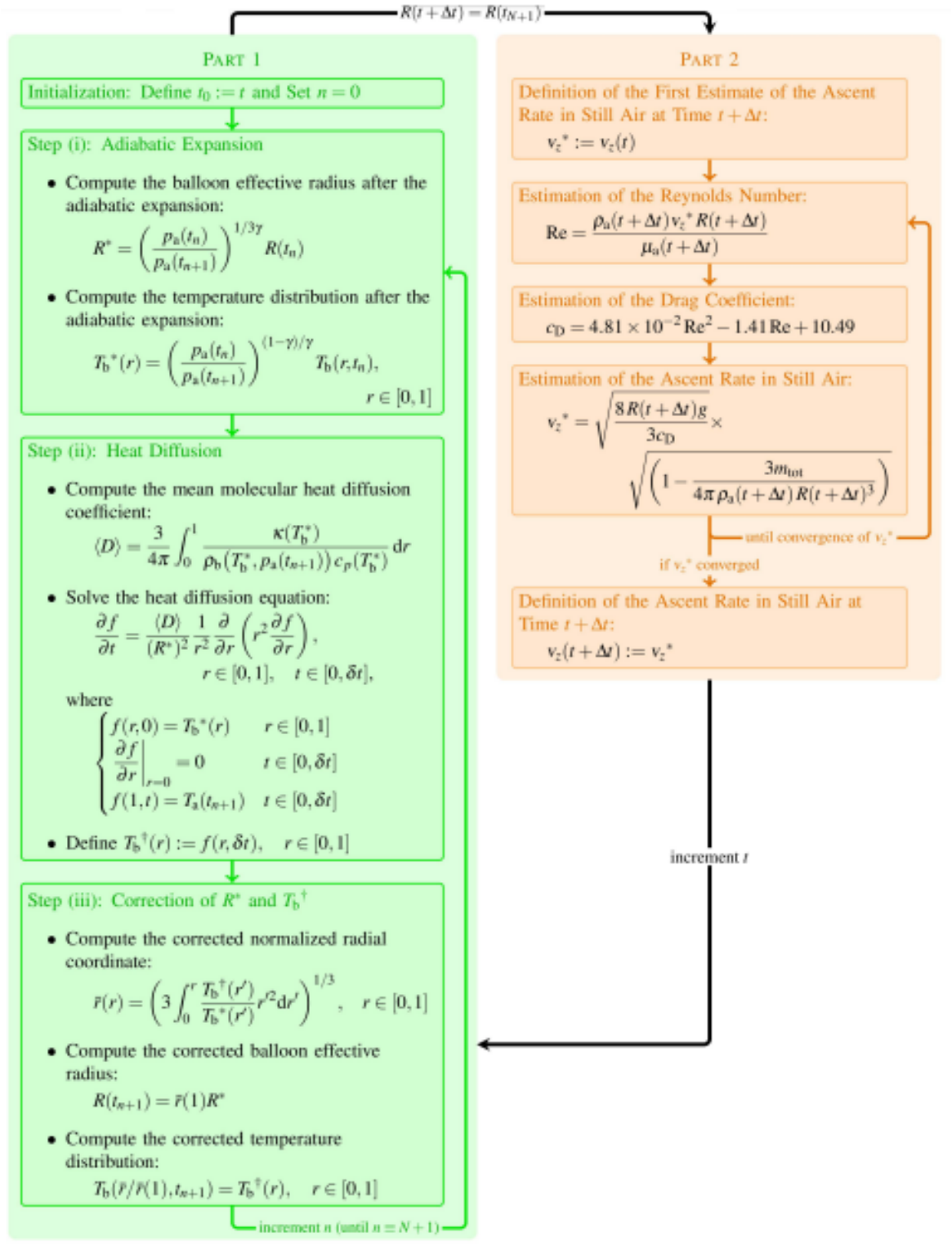

Fig. 3.4. Schematic of the model of the ascent of a balloon in still air

Nevertheless, the model developed for this project will not go through all the steps. The most important reason is the computational cost. Moreover, as it has been mentioned before, it would be necessary to include the fact that there is wind, so no still air assumptions can be done. Instead, the simulator will direcly implement the analytical solution of

Eq. 3.14 with the boundary conditions previously imposed. This solution was computed by Carslow and Jaeger **[4]**:

$$T_b(r,t) = \frac{2}{r}\sum_{n=1}^{\infty}\left(\alpha_n + \beta_n(t)\right) e^{-\bar{D}(\pi n/R^2)t} sin(\pi n r) \ , \tag{3.18}$$

where

$$\alpha_n = \int_0^1 r T_{b,0}(r) sin(\pi n r) dr \ ,$$

$$\beta_n(t) = \frac{\pi D}{R^2} n(-1)^{n+1} \int_0^t T_{out}(s) e^{-\bar{D}(\pi n/R^2)s} ds \ ,$$

and $T_{b,0}$ is the initial temperature inside the balloon, which is assumed to be constant along the radius and equal to the initial outside temperature: $T_{b,0} = T_{out,0}$.

Note that this solution depends on the radius, but since there will be only one temperature sensor inside the balloon, the characteristic radius chosen will be the one at which the sensor is placed: $T_b(r,t) \approx T_b(r \simeq 0.9, t)$.

At this point, there is a missing equation for the evolution of the balloon effective radius. This expression will be presented in the next section.

3.1.4. Material equations

So far, the simulator has included the evolution of the temperature inside the balloon, but without any relation with the variation of the volume. Then it is mandatory to add one equation regarding the increase in radius. Remember that if the steps of the model proposed in the previous section are followed, the increase in radius is part of the solution (see *Figure 3.4*, part 1, step (i)).

The material of the balloon is rubber, which is a hyperelastic material. For any elastic balloon, the envelope exerts a restoring force inwards (Δp); it means that the pressure inside will be a little greater than the pressure outside. The pressure equation is:

$$p_{out} = p_{in} - \Delta p \tag{3.19}$$

where p_{out} will be only function of the altitude of the balloon and p_{in} is given by the ideal gases equation as a function of the temperature inside (T_{in}), the lifting gas (helium) gas constant ($R_g = 2080\ J/kgK$), the number of moles (n) and the current radius (r)[2]:

$$p_{in} = \frac{nR_gT_{in}}{V_b} = \frac{nR_gT_{in}}{\frac{4\pi}{3}r^3} \tag{3.20}$$

The value of n can be computed using the initial conditions.

[2]In comparison with the previous section, here the letter r denotes a magnitude with units: the current radius of the balloon.

Regarding the extra pressure due to the restoring force:

$$\Delta p = 2\frac{h}{r}\sigma_\theta \tag{3.21}$$

where h and r are the current thickness and radius, respectively, and σ_θ is the hoop stress. Depending on the hyperelastic model chosen, the analytical expression of the hoop stress is different. In this project, two models will be implemented in the simulator in order to see which one is closer to the experimental results: Ogden model and Mooney-Rivlin model.

Mooney-Rivlin model

$$\Delta p|_{MR} = 2\mu\frac{h_0}{r_0}\left(\left(\frac{r_0}{r}\right) - \left(\frac{r_0}{r}\right)^7\right)\left(1 + \frac{1-\alpha}{\alpha}\left(\frac{r_0}{r}\right)^2\right) = 0 \tag{3.22}$$

where the shear modulus μ and the parameter α have the typical values for normal rubber **[5]**: $\mu = 300\ kPa$ and $\alpha = 10/11$.

Ogden model

$$\Delta p|_{Og} = 2\frac{h_0}{r_0}\sum_{p=1}^{N}\mu_p\left(\left(\frac{r}{r_0}\right)^{\alpha_p-3} - \left(\frac{r}{r_0}\right)^{-2\alpha_p-3}\right) \tag{3.23}$$

The values of the Ogden parameters are obtained experimentally for each type of material. In the case of normal rubber (and with $N = 3$) **[12]**:

TABLE 3.2. OGDEN PARAMETERS

p	α_p	μ_p $[kPa]$
1	1.3	630
2	5.0	1.2
3	-2.0	-10

The initial radius and thickness of the balloon's envelope are approximately 0.9 m and 0.1 mm, respectively. Accordring to the balloon supplier, the burst radius is $r_f \simeq 2.85\ m$. Knowing this information, the procedure will be to implement together the temperature and material evolution into the simulator and stop when the radius gets the value at burst.

3.2. Experimental procedure

The second part of the project is devoted to validate the model by launching a balloon. In general terms, the system will include: the balloon's envelope, the payload, two antennas (one in the payload to transmit the data, and the other on ground to recieve),

several sensors connected to two Arduinos UNO, three cameras, a radio transmitter, the parachute and a GPS tracker.

The experimental part is divided in several stages:

1. The first step is to buy all the components needed and understand how the whole system will work.
2. Develop the codes in Arduino that will allow the processing of the data acquired by the sensors, and connect the circuits.
3. Build the antenna of the payload.
4. Check that everything works by performing tests.
5. Assembly of all components.
6. Launch the balloon.
7. Analyze the data and compare it with the predictions of the simulator.

3.2.1. Components

In this section, all the parts that are not connected to Arduinos are described.[3]

Balloon's envelope

It is the most important part of the experiment, since it provides the vertical force that allows the system to rise up to the desirable height.

The target altitude of the project is about 30 km (which in fact is the maximum altitude that NOAA provides information about), and the estimated mass of the payload is 2 kg. These two factors lead to a lot of configurations with different materials and weight, but the final option was:

- The material chosen is natural rubber latex, mainly due to the availability of properties and previous researches and experiments, which facilitates the implementation in the simulator.
- The shape of the balloon is spherical, because it is the easiest and cheapest to purchase, as well as because of the simplifications that implies in the simulator.
- The mass of the balloon's envelope is 600 g, mostly because of the cost. In fact, it is close to the lowest balloon's envelope mass that allows us to perform the mission intended.

[3] In the sections 3.2.1 and 3.2.2, parts that are not connected to Arduino are referred to as *Components*, and the parts connected to Arduino, *Electronics*.

Fig. 3.5. Balloon's envelope

Payload box

The payload box is made of polystyrene and its exterior has been painted in bright orange to make it more visible. Its external dimensions are: 22 cm x 22 cm x 19 cm, with a constant thickness of 3 cm. It will contain the electronics and some of the components. Moreover, the payload antenna is placed on its base.

Fig. 3.6. Payload

HD cameras

In order to record the flight, a set of three HD cameras is included: two of them are placed in different lateral faces of the payload, and the remaining one on the top, in charge of recording the burst of the balloon. The type of camera chosen was in terms of the cost and resistance to low temperatures.

Fig. 3.7. Cameras

GPS tracker

This device has two functions:

1. The first and most important one is to help in finding the location of the system once it has returned from the flight. The module must be equiped with a SIM card so that when calling to the number assigned to the card, the device will send back a message with its exact location.
2. The second function is to work as an alternative system able to transmit the position during the flight, in case that the principal system, based on radio communication and two antennas, fails.

Fig. 3.8. GPS tracker

Power supply

The systems will be fed by industrial range batteries (able to work from -40 to 85 ^{o}C), which are mounted on: a battery module that is connected via pins to the Arduinos (two units), and a power bank that is connected via USB to the cameras (three units).

Parachute

It is included in order to avoid the free fall of the system. The parachute by itself has a device that isolates the payload from the torsional moment generated by the parachute and viceversa; however, in case of failure, a carabiner will be included.

Fig. 3.9. Parachute

Lifting gas

Due to its low cost and easy purchase, helium has been chosen as the lifting gas.

Ground antenna

It will receive the encoded data (position of the system) sent by the payload antenna; afterwards, the data will be decoded through an external software. This method will be the main continuous tracking system for the balloon. The chosen model was the Arrow II Satellite Antenna, which is able to receive VHF and UHF.

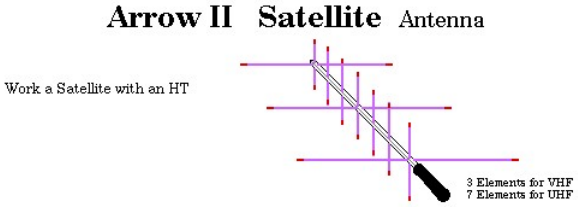

Fig. 3.10. Ground antenna

Others

Ropes and belts that join the balloon's envelope, the payload and the parachute.

3.2.2. Electronics

In this section, all the parts that are connected to the Arduinos are described.

Data processing unit

The data processing unit is a key part of the system since it will allow to process the data acquired by the sensors. The chosen unit was Arduino UNO R3 **[16]** due to the low cost and simplicity with respect to other units, as well as its industrial range. The system will be composed by two Arduinos, each of them in charge of different tasks:

- Recieve and store the GPS data and send it via radio communication through the payload antenna.
- Store the attitude of the payload and the temperature in three different places.

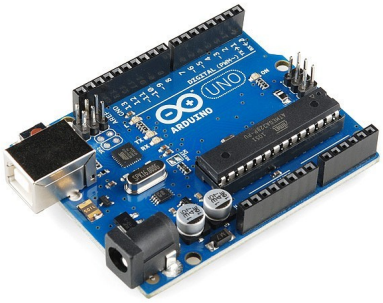

Fig. 3.11. Arduino UNO

GPS unit

The chosen unit was the Adafruit GPS Logger Shield **[17]**, which already includes a SD card reader. The GPS will recieve the position and altitude of the balloon and store it in the SD card.

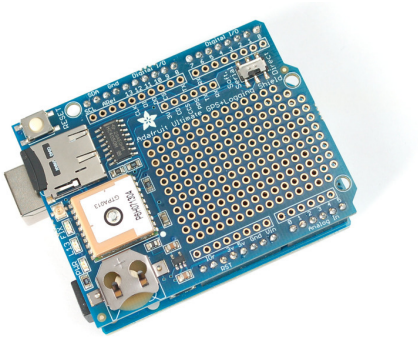

Fig. 3.12. GPS unit

Inertial measurement unit

Although this project is not focused on the attitude of the payload, it is an interesting data to have for future projects that will be able to control the attitude by using an inertia wheel. The IMU chosen was Pololu MinIMU-9 v5 **[18]**, which is a bit more expensive than other units but is compensated with auto-calibration and higher precission.

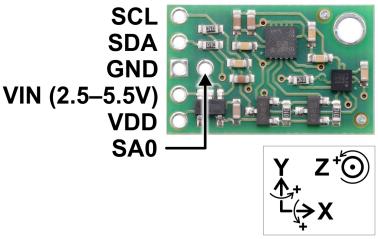

Fig. 3.13. MinIMU-9 v5

Temperature sensors

The model chosen was the DHT22, which has good performance at low temperatures. As it has been mentioned before in the document, the system will include three temperature sensors: one placed outside, one inside the payload and the remaining one inside the balloon. This last one is the most important sensor, together with the GPS: the data acquired by them is essential in order to validate the simulator.

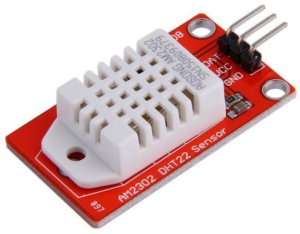

Fig. 3.14. Temperature sensors

Payload antenna

It has been made manually using coaxial cable and single core wire, following the instructions of the webpage: *ukhas.org.uk*. The result is a 1/4 wave antenna with omnidirectional radiation pattern that allows to emit equal radio power in the direcion of all the receivers.

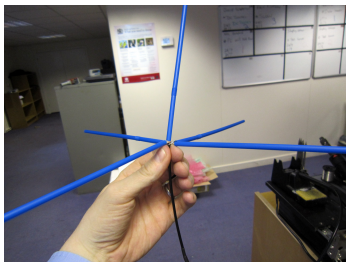

Fig. 3.15. Payload antenna

Radio transmitter

The unit chosen was the NTX2B, which emits at 434.650 MHz (ultra-high frequency). It will be connected to the Arduino with the GPS shield and to the payload antenna, so that the GPS data acquired is coded and sent.

Fig. 3.16. Radio transmitter

SD card reader

Although the GPS unit includes it by itself, it is strictly necessary to store the data processed by the other Arduino, acquired from the temperature sensors, so a SD card reader must be added.

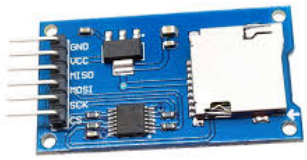

Fig. 3.17. SD card reader

Buzzer

The last electronic part is a buzzer that will emit loud sounds every few seconds when the balloon has crossed 1500 m of altitude during the fall; this will help in the recovery of the system.

Fig. 3.18. Buzzer

3.2.3. Schematic of Arduino

Once all the components and electronics have been defined, the next step is to assembly them to the two Arduinos. In this section the scheme of how the connections look like is

going to be shown.

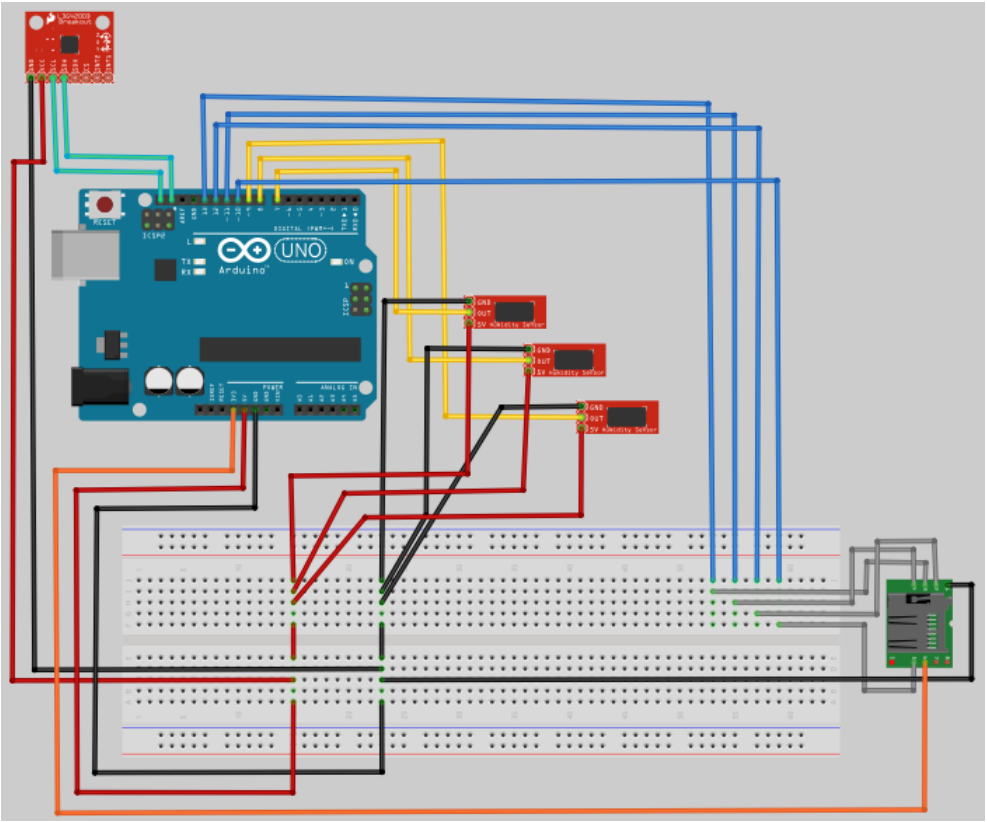

Fig. 3.19. Scheme of the first Arduino

Figure 3.19 displays the scheme of the first Arduino, which includes: IMU, temperature sensors and SD card reader.

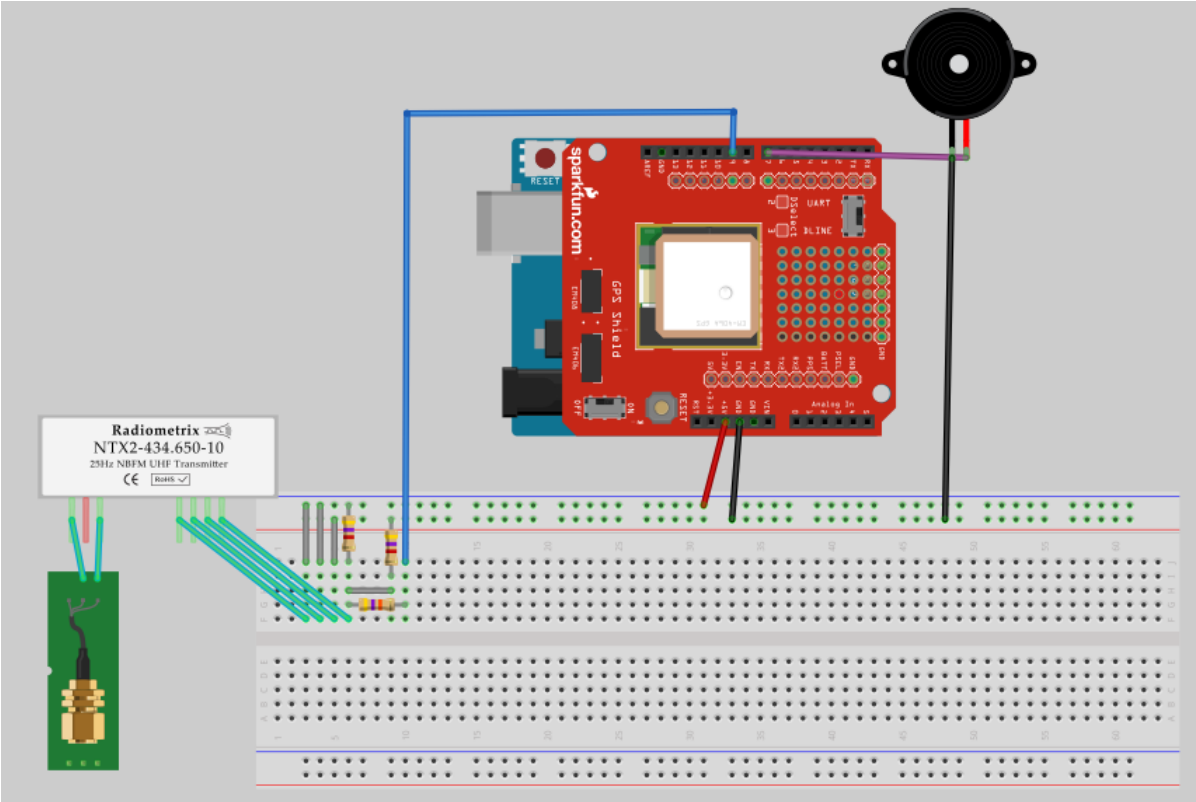

Fig. 3.20. Scheme of the second Arduino

Figure 3.20 shows the scheme of the second Arduino, which includes: GPS, radio transmitter (also connected to the payload antenna) and buzzer.

Note that some components do not coincide with the model bought. The reason is because the program used to make the schemes does not include all the existent electronic components, so a similar one has been used instead. Also, the wiring of both Arduinos was adapted for the components location within the payload enclosure.

3.2.4. Tests

The next and final step prior launch is to verify that everything works, separately and as a whole system. This section is devoted to all the tests performed.

1. Arduino electronics:
   a) Validation of all the components separately (temperature sensors, IMU, GPS, buzzer, etc).
   b) Validation of both Arduinos fully connected.
   c) Refrigerator test to the whole electronic system (in order to ensure that everything works at low temperatures).
2. Communication of the two antennas at long distances.

3. Validation of the parachute.
4. Validation of the GPS tracker.
5. Freezing test to the cameras.
6. Computation of the free-lift; this test is done during the launch, in order to know how much helium is going to be used.

System validation test

In order to validate properly the whole system, an additional test has been performed. It consists on one person receiving data with the gound antenna in a stationary position, and another person carrying the payload around the campus. The idea is to check the precission of the GPS together with the radio communication system.

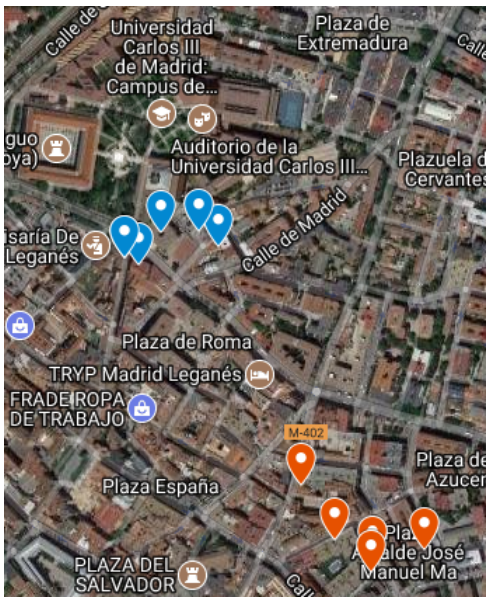

Fig. 3.21. Validation of GPS and communication system

It can be observed in *Figure 3.21* that there are some positions, in orange, that are at an approximate distance of 500 m from the other points. It is due to the necessity of the GPS to fix correctly: it has a transition phase when it is connnected (2 minutes of duration, approximately) in which the measurements are not precise. In fact, the orange positions corresponds to the first data acquired (and sent). The blue positions have an error of about 10 m, which is an acceptable margin.

4. RESULTS

Once the balloon has been launched and the data obtained has been processed, the comparison between the simulator and reality can be done. Due to issues with the experiment, the launch was delayed (from 30th of May to 25th of June) and since the reliable wind data from NOAA is available several days after the day of the prediction, the results will be shown in the presentation.

However, thanks to a collaboration with Mexico University, it is possible to show some results from their launch so that the improvement of the simulator can be noticed.

4.1. Displacement in the horizontal plane

The experimental data corresponds to the results of a launch performed in Mexico (León), the 21^{st} of April. Regarding the simulator, the "new" one refers to the simulator with the temperature and material evolution implemented, while the "old" one is without them.

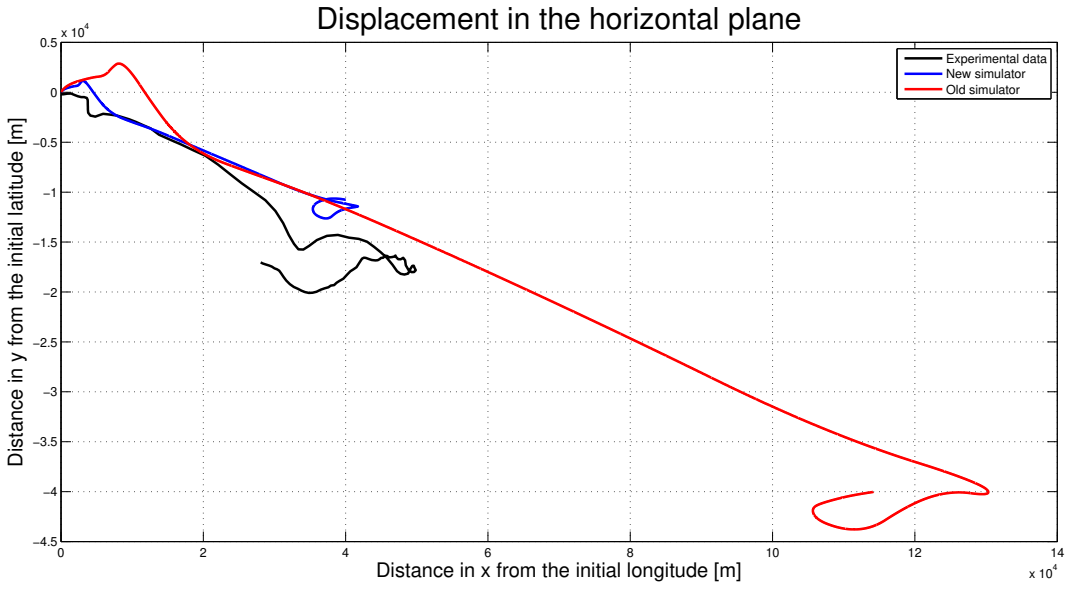

Fig. 4.1. Projection in the horizontal plane of the trajectory

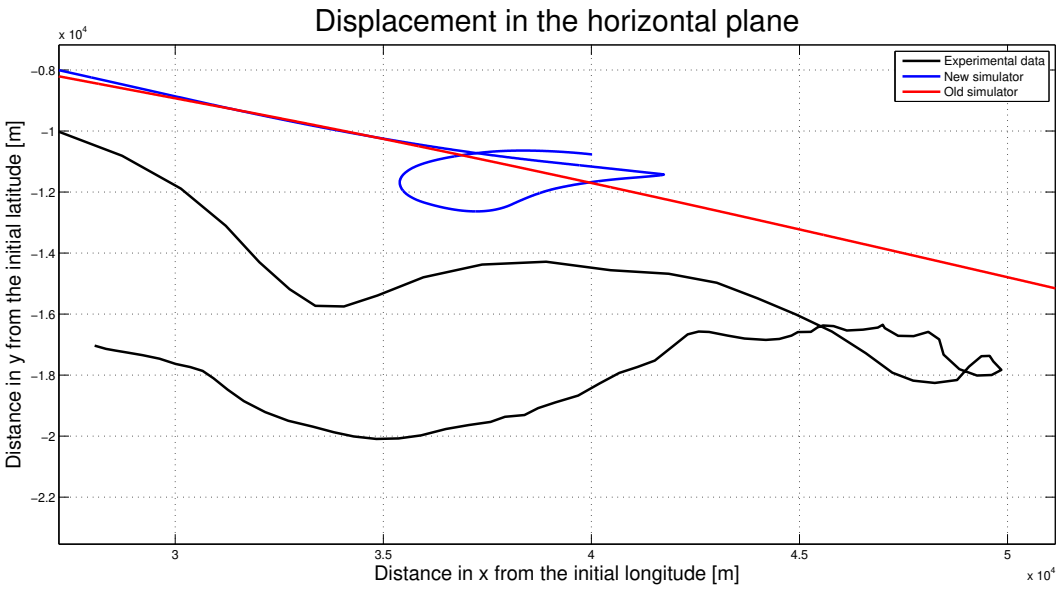

Fig. 4.2. Burst point zoom of the horizontal plane trajectory

As it can be observed in *Figure 4.1*, the addition of the temperature and material equations into the simulator makes it closer to reality, passing from 85.5 km to 11.5 km (approximately) of distance between the predicted and the real burst point.

Although the improvement is huge, the simulator still needs to be more precise. There are two factors that make the experimental results differ from the simulation:

- The first one is external to the simulator itself: the uncertainty of wind cannot be removed, so the data supplied might not be accurate enough. The only way to ensure that this data reduces the uncertainty is by redundancy, using another data supplier and comparing both.
- The assumptions about some parameters and the material models developed in the simulator are not good enough: they make the computational cost lower, but also reduce the approach to reality.

Regarding the comparison between simulators, it makes sense that the addition of both the temperature inside and the radius increase of the balloon improve the results. If the temperature inside is assumed to be equal to the external one, the resultant radius will be smaller, which means a lower balloon's envelope area. Since the drag force is directly proportional to the area, a smaller radius will imply less opposing force to the motion of the balloon, and thus a longer trajectory.

4.2. Altitude evolution

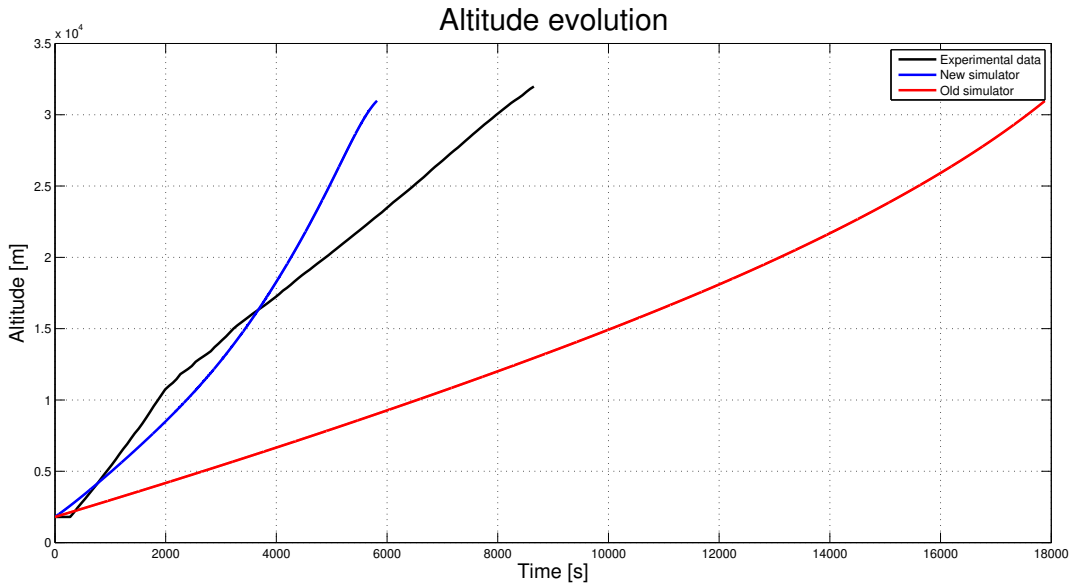

Fig. 4.3. Altitude evolution

In *Figure 4.3* it can be seen again the improvement of the simulator: the difference of time required to reach the burst alttitude between the simulator and the experimental data passes from 2.5 h to 50 min, approximately.

As in the previous section, the assumption of the temperature makes the old simulator predict a smaller expansion, which explains why the balloon reaches the burst altitude sooner in both the experiment and the new simulator.

4.3. Comparison between material models

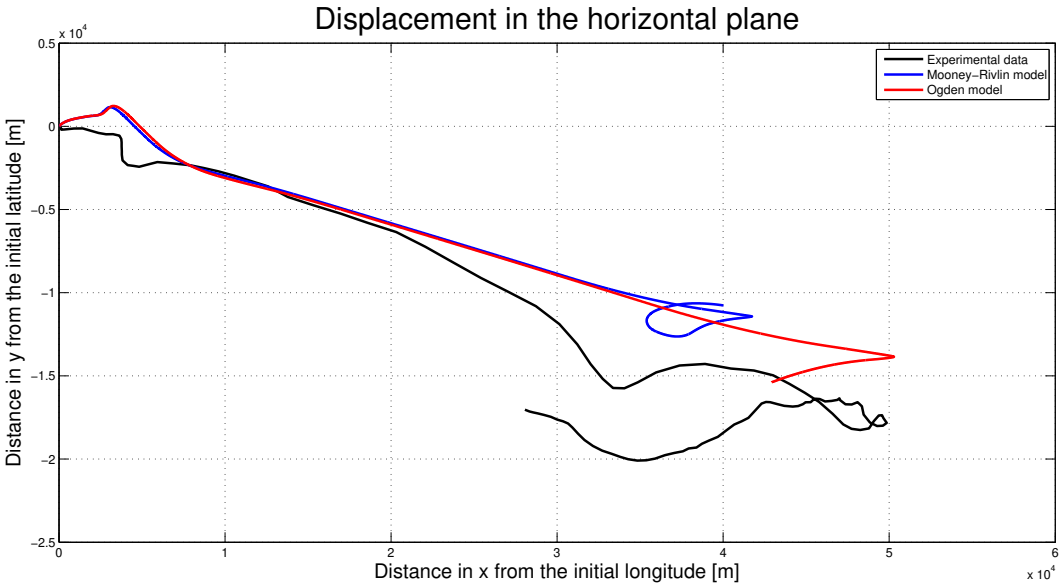

Fig. 4.4. Material model comparison - xy plane

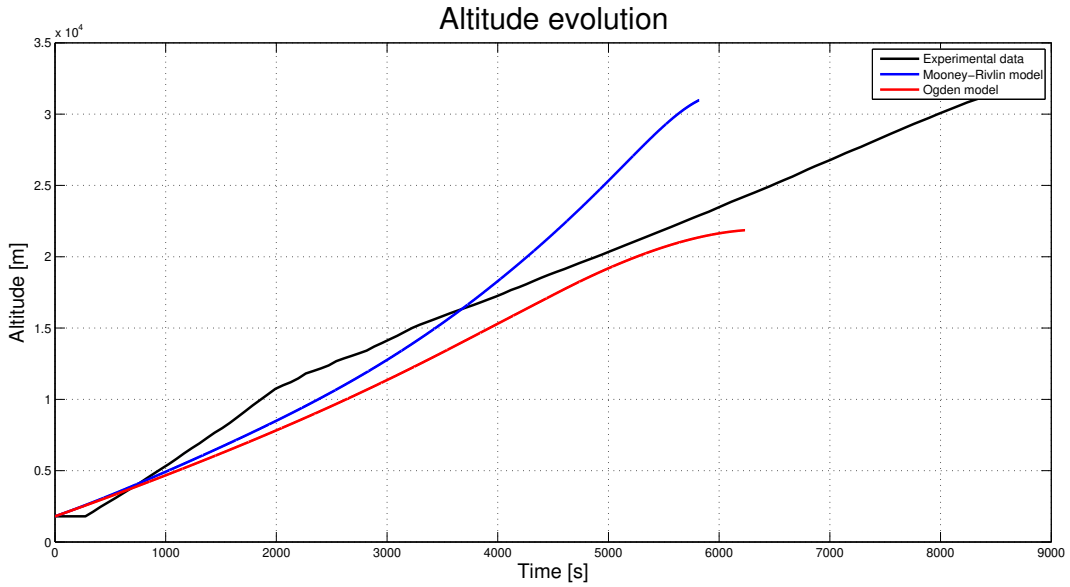

Fig. 4.5. Material model comparison - altitude

In the first graph, *Figure 4.4*, it can be observed that Mooney-Rivlin and Ogden models are very similar during most of the trajectory. However, since according to the Ogden model the balloon ascends slower (*Figure 4.5*), the shift from eastwards to westwards occurs later; thus the burst point is different. The distance from the real burst point to the simulated using Ogden model is around 15 km. Taking into account that this value is 11.5 km for Mooney-Rivlin model, it can be thought that Mooney-Rivlin is better (in

this experiment) than Ogden. However, when comparing the direction change with the experimental data, Ogden model seems to be more precise; the problem comes from the burst altitude calculation. If now *Figure 4.5* is analyzed, the burst altitude according to Ogden model is about 22 km while in both Mooney-Rivlin model and the experimental data, this altitude is 31 km approximately. So regarding the trajectory in the horizontal plane, Ogden model is better, but regarding the burst altitude, Mooney-Rivlin model is closer to reality.

In terms of the computational cost, Mooney-Rivlin model can be solved as a high-order polynomial, while Ogden model needs a non-linear equation solver (remember that both of them are coupled with *Eq. 3.18*). This makes Mooney-Rivlin model more computational cost effective, so it would be the preferred option for future simulations.

5. IMPROVEMENTS OF THE PROJECT

The improvements of the project can be divided in three groups: those regarding the experiment, those regarding the simulator and those involving both parts.

Regarding the experiment, it is very important to optimize the system, since higher quality is direclty related with a better performace, meaning less probability of failure and more complex systems. The possible improvements of the experiment for future launches are described next:

- The first improvement is related with the processing unit. Even though the price, robustness and simplicity of Arduino make it ideal for this project, as the missions become more complex, the need for a more sophisticated system begins to be important. A good substitute would be Raspberry Pi.

- Although a balloon's envelope of 600 g is cheaper than bigger ones and it was enough to perform the experiment, it limited the ascent velocity for the mass of the payload required. Thus, a nice change would be to use a bigger balloon: it will not only allow to perform the flight in less time (due to higher vertical velocity), but also to reach higher altitudes. Also, if a totally functional super-pressure balloon system is intended to be developed, the shape of the balloon's envelope would need to be different (from spherical shape to natural-shape).

- Another important issue was the mass of the payload; approximately 80% came from the batteries: four for each Arduino plus four for each camera, which makes a total of 20 batteries. The decrease in the amount of batteries used would imply the possibility to add more devices such as a wheel of inertia which is able to rotate the payload through remote control from the ground. One possibility is to substitute the industrial batteries by solar panels since the mission is intended to be performed during daytime. Furthermore, depending on the purpose of the mission, some cameras can be removed: for instance, if the aim is related with surveillance, the camera in the top can be taken away.

Regarding the simulator, if the final purpose is to make a fully functional balloon-based system (e.g. for the applications mentioned in the section of *Future applications*), a more precise model will be required. The first improvements that the simulator should include are specified next:

- One of the first assumptions of the model was related with the non-dimensional coefficients C_Y and C_D. In the case of C_Y, it was assumed to be zero because of the spherical shape of the balloon, which can be further assumed as long as the type of balloon remains unchanged. But for C_D, as it has been seen in *Figure 3.2*, it has a

strong dependency on the Reynolds number and the turbulence of the air. If larger balloons and/or higher ascent velocities are the natural evolution of this project, then it will be mandatory to take into account how the drag coefficient varies.

- Regarding the temperature inside the balloon, since there was only one temperature sensor, the *Eq. 3.18* was computed for $r = 0.9$, and this result was the one used to calculate the volume enclosed by the balloon (*Eq. 3.13*). The next step in the simulator is to take into account the whole temperature distribution in order to compute the volume more accurately.

- In order to have a relation between the temperature inside and the radius of the balloon, two models were developed: Mooney-Rivlin and Ogden. All the models are based on experiments, and the coefficients used correspond to normal rubber, so in order to have more precise results, the parameters should be taken for the exact same material as the balloon's envelope. Furthermore, it would be interesting to explore more models, such as Gent, Yeoh or Arruda-Boyce.

- Although NOAA provides average wind predictions, based on probability to occur, it can fail in a given day or altitude. In order to be sure that the prediction is correct, an additional wind data supplier is intended to be consulted; in this way, by redundancy, the probability of a wrong wind prediction will decrease drastically. Moreover, sometimes, the webpage of NOAA stops giving free access to its data during a couple of days, so the idea of redundancy becomes more important.

- Once a reliable simulator of the ascent of a balloon has been developed, the next step is to model the falling. In this way, the prediction (and also optimization) of the whole trajectory of the balloon, from the launch to the landing point, could be done.

Finally, there are two issues that would imply the improvement of both the experiment and the simulator: control system and super-pressure.

5.1. Control system

It is one of the most important improvements since it will allow to fly the balloon at the desired altitude. Although the lateral control is also an interesting issue, it will be assumed to be performed in the same way that Project Loon works: knowing the direction and velocity of the wind in the different layers of the stratosphere, the relevant task is to put the balloon in the correct altitude.

The most used altitude control systems are based on a high pressure gas chamber that is able to inject or extract gas inside the balloon. In this system, two valves are required in order to control the gas flow, which means that the mass of the gas will vary depending

on these two valves:

$$\frac{dm_g g}{dt} = -\rho_g(e_1 + e_2) \ , \tag{5.1}$$

where

$$e_1 = c_1 A_1 \sqrt{\frac{2\Delta p_1}{\rho_g}} \tag{5.2}$$

$$e_2 = c_2 A_2 \sqrt{\frac{2\Delta p_2}{\rho_g}} \tag{5.3}$$

In these equations, subscript 1 refers to the venting valve while subscript 2 is related to the exhaust valve. The term e is the volumetric rate, A is the cross-sectional area and c is the flow rate constant, that is computed by multiplying the flow contraction coefficient and the rate coefficient of the valve.

Another popular technique to increase the altitude of the balloon consists in a ballast system: whenever the balloon needs to go to a higher layer, some mass is dropped. There are two problems with this system: the mass dropped cannot be reincorporated, so the ballast system can only be used to go in one direction (ascend, never descend); the other problem is related with the precission of the system.

The equation that the model should incorporate in order to take into account a ballast system is similar to the equations of the valves, but in this case all the balloon system mass varies:

$$\frac{dm_c}{dt} = -e_3 \ , \tag{5.4}$$

where e_3 refers to the mass dropp rate of the ballast.

5.2. Super-pressure

A super-pressure balloon is a non-extensible envelope that is able to withstand differentials in pressure (as it was mentioned in the section *Material equations* of the *Methodology*, pressure inside is higher than outside), taking into account the night cycle. Moreover, this type of balloon does not need a ballast system to maintain the altitude.

The key factor of super-pressure balloons is the material: it has to be high pressure resistant and light enough. Combining these two characteristics is extremely difficult, and since the beginning of modern ballooning it has been a subject of research. The way of developing a successful super-pressure balloon is divided in two aspects:

- The first one is by simply using a material with the properties mentioned in the previous paragraph. The materials that present the best performance are: saran-polyethylene laminate, mylar-polyethylene laminate and polyethylene impregnated fiberglass.

- The second aspect is related to the shape of the balloon, being the natural-shaped the best choice. Natural balloon shape is a rotationally symmetrical body made only of film; this shape increases the resistance to pressure of the envelope, which makes it ideal to super-pressure balloons.

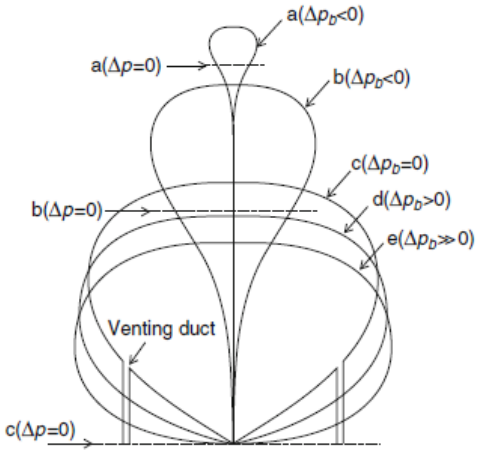

Fig. 5.1. Natural-shape balloon

6. CONCLUSIONS

During this project the relevance of balloons in several fields, such as meteorology, has been shown: the low cost of a launch compared with other systems makes high-altitude balloons a nice choice in order to simulate near-space conditions; at lower altitudes, the floating capability in addition to long flying times make balloons the perfect system for surveillance.

Most of applications of weather balloons are based on a super-pressure system and/or include altitude control. Both of them are the next step of this project: once the simulator is able to predict with minimum error the trajectory of a balloon, first an altitude control will be added, and then, if possible, the super-pressure.

Taking into account the importance of balloons, it is crucial to be able to simulate properly the flying path that a balloon is going to perform prior its launch. Although the assumption regarding the temperatures ($T_{in} = T_{out}$) simplifies substantially the simulator, it is not a good hypothesis because in rubber balloons, the difference expected is of the order of tenths of Kelvin. Thus, the addition of the temperature model is essential for the simulator.

Regarding the material evolution, two models have been developed: Mooney-Rivlin and Ogden. Both of them are based on experimental results, so they contain some parameters that are characteristic for each material. It is necessary to ensure that the material of the balloon's envelope is exactly the same as the experimental procedure that determines those parameters.

Finally, the uncertainty of the wind predictions cannot be avoided. The lack of an additional wind data supplier can make the results differ from reality, even though the simulator implements the physical laws governing the system accurately enough.

BIBLIOGRAPHY

[1] N. Yajima, T. Imamura, N. Izutsu and T.Abe. *Engineering Fundamentals of Balloons*, Springer New York, New York, NY, 2009, pp. 15-75.

[2] James A. Armstrong, Philip A. Russell, Leslie E. Sparks and Dennis C. Drehmel. *Tethered Balloon Sampling Systems for Monitoring Air Pollution*, Journal of the Air Pollution Control Association, 13 March 2012.

[3] Google. *Google's project Loon*.

[4] H. Carslaw and J. Jaeger. *Conduction of heat in solids*, Clarendon Press, 2nd Edn., 1959.

[5] Ingo Müller and Peter Strehlow. *Rubber and rubber balloons: paradigms of thermodynamics*, Lecture Notes in Physics, Springer, 2004.

[6] L.R.G. Treloar. *The Physics of Rubber Elasticity*, 2nd Edn. Glasgow: Oxford University Press, 1958.

[7] S.A. Rinehart, M. Rizzo, D.J. Benford, D.J. Fixsen, T.J. Veach, A. Dhabal, D.T. Leisawitz, L.G. Mundy, R.F. Silverberg, R.K. Barry, J.G. Staguhn, R. Barclay, J.E. Mentzell, M. Griffin, P.A.R. Ade, E. Pascale, G. Klemencic, G. Savini and R. Juanola-Parramon. *The Balloon Experimental Twin Telescope for Infrared Interferometry (BETTII): An Experiment for High Angular Resolution in the Far-Infrared*, Publications of the Astronomical Society of the Pacific, Vol. 126, No. 941 (July 2014), pp. 660-673.

[8] R.P. Murphy1, M. Sasaki, W.R. Binns1, T.J. Brandt, T. Hams, M.H. Israel, A.W. Labrador, J.T. Link, R.A. Mewaldt, J.W. Mitchell, B.F. Rauch, K. Sakai2, E.C.Stone, C.J. Waddington, N.E. Walsh, J. E. Ward and M.E. Wiedenbeck. *Galactic cosmic ray origins and OB associations: evidence from SuperTIGER observations of elements 26Fe through 40Zr*, 29 August 2016.

[9] National Aeronautics and Space Administration. *Eclipse Balloons*.

[10] Luke W. Renegar. *A Survey of Current Balloon Trajectory Prediction Technology*, University of Maryland, College Park, MD, 20742.

[11] J. Snowman, A. Greig and D. Richman, "Cambridge University Spaceflight Landing Predictor", 2013; URL: predict.habhub.org.

[12] R.W. Ogden. *Elastic deformation of rubberlike solids*, The Rodney Hill 60th Anniversary Volume, Pergamon Press, 1982.

[13] C.A. Authority. *Sera, air navigation order 2009 and rules of the air regulations 2015 - consolidation*, 18 March 2016.

[14] FAA. *Faa part 101-moored balloons, kites, amateur rockets, unmanned free balloons, and certain model aircraft*, 14 June 2017.

[15] A. Gallice, F.G. Wienhold, C.R. Hoyle, F. Immler and T. Peter. *Modeling the ascent of sounding balloons: derivation of the vertical air motion*, 20 October 2011.

[16] Arduino. *Arduino characteristics*.

[17] Adafruit. *Adafruit gps overview*.

[18] Pololu. *MinIMU-9 v5 Gyro, Accelerometer, and Compass (LSM6DS33 and LIS3MDL Carrier)*.

[19] Gobierno de España. *Gobierno de España, disposición 542 del boe num. 15 de 2017, ministerio de la presidencia*, January 2017.

[20] Guillermo M. Asensio López, *Dynamic Modelling, Simulation, and Control of an Atmospheric Balloon Platform*, Bachelor Thesis, Department of Aerospace Engineering, Universidad Carlos III de Madrid, June 2017.